

Oblate Electron Holes are not attributable to Anisotropic Shielding

I H Hutchinson

Plasma Science and Fusion Center,
Massachusetts Institute of Technology,
Cambridge, MA, USA.

Abstract

Shielding mechanisms' influence on the ratio of perpendicular to parallel scale lengths of multidimensional plasma electron hole equilibria are analyzed theoretically and computationally. It is shown that the “gyrokinetic” model, invoking perpendicular polarization, is based on a misunderstanding and cannot explain the observational trend that greater transverse extent accompanies lower magnetic field. Instead, the potential in the wings of the hole, outside the region of trapped-electron depletion, has isotropic shielding giving $\phi \propto e^{-r/L}/r$, with the shielding length L equal to the Debye length for holes much slower than the electron thermal speed. Particle in cell simulations confirm the analysis.

1 Introduction

Plasma electron holes[1] are widely observed by satellites in space. They are a major subset of the various observed Electrostatic Solitary Wave (ESW) structures that are important elements of the plasma turbulence in various regions. They move along the magnetic field (B) at speeds a fraction of the electron thermal speed, thus suppressing the (slower) ion response (which will be ignored here), and are sustained by a deficit of electrons on trapped orbits: a kind of Bernstein-Greene-Kruskal (BGK) mode. Although one-dimensional BGK analysis[2] seems to provide an understanding of the parallel (to B) structure, electron holes are frequently observed to be two- or three-dimensional: of limited transverse extent. It has been shown computationally [3, 4] and explained with quantitative analysis [5–7] that so-called transverse instabilities break up one-dimensional holes into smaller transverse length scales. And, increasingly, multi-satellite (e.g. Cluster[8] and MMS[9, 10]) observations are documenting the transverse potential structure. It therefore seems essential to develop a multi-dimensional understanding of their equilibria and stability, in order to understand the observations and simulations. The purpose of this paper is to rule out from consideration a much cited but erroneous hypothesis proposed to explain the multi-dimensional shape of electron holes; and hence to indicate more narrowly what mechanisms could be important.

In their pioneering observations, using the Polar satellite, Franz et al[11] represented the shape of electron holes by the ratio of scale lengths L_{\perp}/L_{\parallel} , perpendicular and parallel to the magnetic field. They found that between 1.8 and 9 earth radii, weaker magnetic field regions of the magnetosphere had holes that were statistically more oblate: more elongated in the directions perpendicular to the magnetic field. They fitted their results as $L_{\perp}/L_{\parallel} \simeq \sqrt{1 + \omega_p^2/\Omega^2}$, where ω_p is the plasma frequency, and Ω the (electron) cyclotron frequency. They also offered a speculation that the reason for this scaling is to be found in a “modified” Poisson equation of the form

$$\left[\nabla_{\parallel}^2 + \left(1 + \frac{\omega_p^2}{\Omega^2}\right) \nabla_{\perp}^2 \right] \phi = -\rho_s/\epsilon_0, \quad (1)$$

which in the context of the “gyrophase averaged Vlasov equation”, arises “to include the polarization density of the particles”. They referenced early papers[12, 13] relating to what is now called gyrokinetics, a reduced model much used for low frequency turbulence studies. This explanation has been taken up by several subsequent authors in electron hole research[4, 14–20], often being approvingly called the gyrokinetic scaling relation.

If this model really applied to electron holes, its effects would be a vital part of multi-dimensional equilibria. However, it does not, because it misunderstands gyrokinetics. The phenomenon of transverse polarization *cannot provide the explanation* of the observed hole aspect ratio scaling because its contribution is always small, as is now explained.

2 Transverse plasma polarization

2.1 Elementary derivation

Transverse polarization is discussed in text books. Addressing just the motion of electrons (charge q , mass m , density n_e), the particles drift in response to perpendicular electric fields via the $\mathbf{v}_{E \times B} = \mathbf{E} \times \mathbf{B}/B^2$ drift and, in a time dependent $\mathbf{v}_{E \times B}$, polarization drift: $\mathbf{v}_p = \frac{m}{qB^2} \dot{\mathbf{E}}_{\perp} = -\frac{m}{qB^2} \nabla_{\perp} \dot{\phi}$ arises from inertial force. Integrating \mathbf{v}_p with respect to time, the displacement gives an electric polarization density

$$\mathbf{P} = qn_e \int \mathbf{v}_p dt = -\frac{n_e m}{B^2} \nabla_{\perp} \phi = -\epsilon_0 \frac{\omega_p^2}{\Omega^2} \nabla_{\perp} \phi \quad (2)$$

where $\Omega = |q|B/m$ and $\omega_p^2 = n_e q^2/\epsilon_0 m$.

If, then, there exists a specified charge density ρ_s that somehow excludes the electron polarization response, so in terms of elementary dielectric theory it is a “free-charge-density”, yet resides in an electron plasma in which *the only electron response is the polarization drift*, the potential will be governed by Poisson’s equation containing, in addition to ρ_s , a polarization charge density $\rho_{\epsilon} = -\nabla \cdot \mathbf{P} = \epsilon_0 \frac{\omega_p^2}{\Omega^2} \nabla_{\perp}^2 \phi$. Hence, Poisson’s equation $-\nabla^2 \phi = (\rho_s + \rho_{\epsilon})/\epsilon_0$ can be written in the modified form of equation (1): $\left[\nabla_{\parallel}^2 + \left(1 + \frac{\omega_p^2}{\Omega^2}\right) \nabla_{\perp}^2 \right] \phi = -\rho_s/\epsilon_0$. This is equivalent to saying that the polarization drift gives rise to an anisotropic (relative) dielectric tensor $\epsilon = \mathbf{I} + (1 + \omega_p^2/\Omega^2)(\mathbf{I} - \hat{\mathbf{z}}\hat{\mathbf{z}})$, where $\hat{\mathbf{z}}$ is the magnetic field direction.

Some electron hole papers suppose that the anisotropy should be scaled away by defining new transverse spatial coordinates $(x', y') = (1 + \omega_p^2/\Omega^2)^{-1/2}(x, y)$ leading to isotropic solutions in the new coordinates, depending only on $r' = \sqrt{x'^2 + y'^2 + z^2}$, which on this assumption would give Franz's L_\perp/L_\parallel scaling. But this is a mistake because the treatment has implicit approximations not satisfied for electron holes, and ignores the general properties of untrapped collisionless orbits in a potential well.

2.2 The dielectric response in gyrokinetics

The gyrokinetic approximation is based on an ordering that takes the perturbation to be slowly varying both intrinsically as $|\frac{\partial}{\partial t}| \simeq \omega \ll \Omega$ and convectively along the magnetic field as $k_\parallel v_t \ll \Omega$. Gyrokinetics' strength (in modern formulations) is that (unlike the derivation just given and the references cited by Franz) it does not necessarily assume the gyro-radius r_L to be small compared with the transverse perturbation scale. For $k_\perp r_L \gtrsim 1$ one must average over the gyroradius, as if the gyrating particle were a ring of charge on its approximately circular transverse orbit. Also, since gyrokinetics is generally expressed as the motion of the gyrocenter, its Poisson equation (for an electrostatic problem) requires a transformation from gyrocenter-density, back to particle-density, which is what determines the local charge density and potential. This is where the polarization drift enters. Actually gyrokinetic analyses often replace Poisson's equation with quasineutrality, and address the ion polarization more than the electron polarization, neither of which is appropriate for electron hole analysis. The electron polarization is the question here, but is to be dealt with using the same analysis as in standard gyrokinetics for the density of the ions.

A helpful discussion of the resulting transverse dielectric constant and its relationship to what is known about the full dielectric response without gyrokinetic approximations is found in reference [21]. From that paper the electron contribution important for holes can be drawn by extension of their ion analysis. The effective electron gyrokinetic transverse (relative) dielectric constant expressed in Fourier space is

$$\epsilon_\perp = 1 + \frac{1}{k^2 \lambda_{De}^2} (1 - \Gamma_0(b)) \quad (3)$$

$$\simeq 1 + \left(\frac{k_\perp}{k}\right)^2 \left(\frac{\omega_{pe}}{\Omega}\right)^2 \quad (b = k_\perp^2 r_L^2 \ll 1) \quad (4)$$

$$\simeq 1 + \left(\frac{\omega_{pe}}{\Omega}\right)^2 \quad (k_\parallel/k_\perp \ll 1), \quad (5)$$

where λ_{De} is the electron Debye length, and $\Gamma_0(b) = e^{-b} I_0(b)$, with $b \equiv k_\perp^2 T/\Omega^2 m$ the thermal value of $k_\perp^2 r_L^2$. A small- b expansion has $\Gamma_0(b) \simeq 1 - b$, which is the basis for the first approximation in this sequence [eq. (4) noting that $\omega_{pe} \lambda_{De} = \sqrt{T/m}$]. However using it for $b \gtrsim 1$ gives completely the wrong dependence since as $b \rightarrow \infty$, $\Gamma_0(b) \rightarrow 1/(2\pi b)^{1/2}$ remaining positive. A somewhat better (Padé) approximation[22] $\Gamma_0(b) \simeq 1/(1+b)$, avoids so egregious an error, giving $1 - \Gamma_0 \rightarrow 1$ as $b \rightarrow \infty$, the unmagnetized result. The electron hole elongation model explanation requires eq. (5) to apply into the regime where $\omega_{pe}/\Omega = r_L/\lambda_{De} \gg 1$. Since electron holes have $k \sim 1/\lambda_{De}$, it never does. Instead, at weak magnetic field the large- b limit applies: $\epsilon_\perp \rightarrow 1$.

Summarizing: the so-called gyrokinetic model to explain electron hole transverse extent is mistaken because in the regime $\omega_{pe} \gtrsim \Omega$, where the polarization term is relevant, (1) gyrokinetics does not apply to electron holes because their parallel length is too short ($k_{\parallel} v_t \not\ll \Omega$); (2) Franz's expression (5) uses an approximate form for the gyrokinetic dielectric response in a regime where it is invalid; and (3) polarization drift is not the only electron response, as will now be discussed.

3 Density in a general attractive potential

An independent demonstration of the point can be derived from far more general considerations, and these also bear directly on the existence of multidimensional hole equilibria. A collisionless multi-dimensional electron hole (attractive electrostatic potential) time-invariant in some frame of reference moving along the uniform magnetic field, has electron populations that are either trapped or untrapped. The effect of an electrostatic structure like this on the density of the attracted species is a general matter long studied for electric probes and other plasma perturbing bodies[23–25]; the present case differs only in that there is no particle absorption by a body — a simplification. Any point in phase-space is on either a trapped or untrapped orbit.

Henceforth we use normalized units λ_{De} for length, $1/\omega_{pe}$ for time, the background temperature $T_{e\infty}$ for energy, and express densities normalized to the distant background electron density $n_{e\infty}$; the electron mass is then unity and charge -1 . In steady state, the total energy $W = v^2/2 - \phi$ (normalized units) of a particle is conserved, and in collisionless situations, the distribution function is conserved along orbits. Therefore on any untrapped orbit at potential ϕ the (3-D) distribution function is $f(v) = f_{\infty}(v_{\infty})$, the distant (assumed uniform) distribution f_{∞} at the velocity $v_{\infty} = \sqrt{2W}$ ($\phi_{\infty} = 0$). All untrapped orbits will be populated at this level, and if the trapped phase-space is negligible, a simple Boltzmann factor density dependence is the outcome. The *trapped* orbits' distribution, by contrast, is not determined in this way by boundary conditions, and requires consideration of initial conditions or weak collisions[26, 27].

In cylindrical or spherical symmetry situations, determining which orbits are trapped is considerably complicated by the conservation of corresponding angular momentum or z -momentum (for z -ignorable). However, in a multidimensional electron hole, in which cylindrical angle θ is the only possibly ignorable coordinate, the only exactly conserved quantity in addition to energy is the canonical angular momentum p_{θ} which mostly restricts the radial ($x^2 + y^2$) excursion, and does not prevent orbits from escaping the potential well along the magnetic field, in the z -direction. Therefore orbits of positive total energy (W) are trapped only when the magnetic moment ($\mu = mv_{\perp}^2/2B$) is adiabatically conserved, and the resulting conservation of parallel energy $W_{\parallel} = \frac{1}{2}v_{\parallel}^2 - \phi$ causes parallel trapping if W_{\parallel} is negative. When μ conservation is violated because the gyroradius is comparable to the hole's size, the parallel trapping begins to break down and eventually the only trapped particles are those with negative total energy W .

If the *only trapped* orbits are those with negative *total* energy $W = v^2/2 - \phi < 0$, then the untrapped density is $n_u = \int \int_{v_m}^{\infty} f_{\infty}(v_{\infty}) v^2 dv d\Omega_s$, where $v_m = \sqrt{2\phi}$ and $d\Omega_s$ is the solid angle element. For an unshifted 3-D Maxwellian distant distribution, $f_{\infty}(v) =$

$(2\pi)^{-3/2} \exp(-v_\infty^2/2)$, the untrapped density expression can be integrated by parts using $v_\infty^2 = v^2 - v_m^2$:

$$n_{3u} = \frac{4\pi}{(2\pi)^{3/2}} \int_{v_m}^{\infty} \exp([v_m^2 - v^2]/2) v^2 dv = \frac{2}{(2\pi)^{1/2}} \left\{ v_m + \int_{v_m}^{\infty} \exp(-v_\infty^2/2) dv \right\}. \quad (6)$$

This should be compared with the 1-D density of particles that are not *parallel* trapped when v_\perp and $\frac{1}{2}v_\parallel^2 - \phi$ are conserved, those with $W_\parallel > 0$, which is:

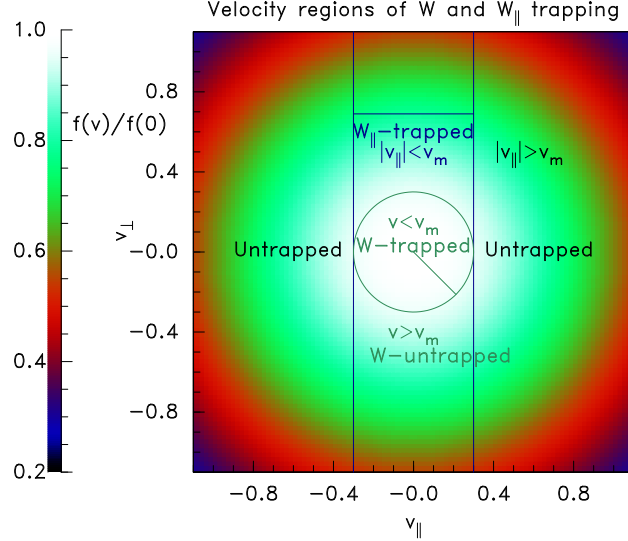


Figure 1: Schematic of the total-energy-trapped and parallel-trapped regions in velocity space.

$$n_{1u} = 2 \int_{v_m}^{\infty} f_\parallel dv_\parallel = \frac{2}{(2\pi)^{1/2}} \int_{v_m}^{\infty} \exp(-v_\parallel^2/2) dv_\parallel. \quad (7)$$

The velocity domains of these two types of untrapped density are illustrated in Fig. 1. There is far more phase space volume subject to parallel trapping (when W_\parallel is conserved) than to total energy trapping. The difference in the densities, $(n_{3u} - n_{1u}) = 2v_m/\sqrt{2\pi}$, is exactly equal to the contribution from the (W_\parallel) -trapped region to density in a one-dimensional hole when the trapped distribution is flat $f_{\parallel t} = f_{\parallel \infty}(0)$. We denote the total density (trapped plus untrapped) of this flat-trapped distribution as n_{1f} , and have $n_{3u} = n_{1f}$. It can easily be shown that n_{3u} and $n_{1f} \simeq 1 + \phi$ to lowest order in ϕ . (For *shifted* Maxwellian distributions the coefficient of ϕ becomes gradually smaller, the shielding weaker[1, Fig 10], but the generalization is straightforward, and the shielding remains isotropic.) Therefore, even if the entire $W < 0$ trapped velocity-region were completely depleted of electrons (making n_{3u} the total density) that would be insufficient to make the electron density *decrease with* ϕ or give a positive charge density for small ϕ . This is the qualitative reason[1, 28] why multidimensional electron holes cannot exist without a magnetic field. Any density contribution (or deficit) from the $W < 0$ region of phase space is of the form $n_{3t} = 4\pi v_m^3 \langle f_t \rangle / 3 = 4\pi(2\phi)^{3/2} \langle f_t \rangle / 3$,

which enters as a higher power $\phi^{3/2}$ than in $n_{3u} - 1(\propto \phi)$, justifying 3D Debye shielding ($n - 1 = \phi$) in the small ϕ limit, regardless of trapped density.¹

In summary, an assumption that orbits are trapped if and only if the total energy is negative, $v^2/2 - \phi < 0$, gives rise, at lowest order, to a Debye shielding density $n \simeq 1 + \phi$, with an isotropic Poisson equation $\nabla^2 \phi = \phi$, and no additional $(\omega_p/\Omega)^2$ term, regardless of trapped distribution. This situation is the anticipated result of small magnetic field, for which the gyro-radius $r_L \sim v_\perp/\Omega$ is much bigger than the potential structure extent L .

On the other hand strong magnetic field, $r_L \ll L$ with $L \sim \lambda_{De}$ makes the term $(\omega_p/\Omega)^2 = (r_L/\lambda_D)^2 \sim (r_L/L)^2$ negligibly small, again yielding an isotropic effective Poisson equation. In this limit parallel trapping predominates, and Debye shielding is recovered only by taking the shielding distribution to include a flat contribution $f_{||t} = f_\infty(0)$ in the trapped velocity region: in other words the electron deficit that sustains the hole is the difference $f_{||} - f_{||\infty}(0)$ in the trapped phase-space.

In the intermediate regime, $(\omega_p/\Omega)^2 \sim 1$, whether an orbit is or is not trapped cannot be decided simply, because magnetic moment approximate conservation depends upon subtleties of orbit velocity. But the trapped region in phase-space is certainly intermediate between the two extremes of total-energy and parallel-energy trapping. Therefore it can hardly be expected that the untrapped density will be suppressed significantly below $1 + e\phi/T$, as would be implied by use of eq. (1). These conclusions are consistent with our discussion of gyrokinetics.

4 Particle in Cell Confirmation

A simple way to confirm the analytic conclusions arrived at here is to perform full orbit, 6-dimensional phase-space, particle in cell (PIC) simulations. The COPTIC code[29] is used which is capable of imposing a potential boundary condition embedded within the plasma. A cube of plasma with sides extending to ± 6 (Debye lengths) is used with a uniform magnetic field in the z -direction. Potential is represented on a 60^3 mesh with domain boundary conditions $\partial\phi/\partial|x| = -\phi$ (and similarly for y and z) although the exact form is not observed to be important. The (~ 4 million) particles move periodically at the transverse boundaries x, y , but the z boundaries are open with particles reinjected representing an external Maxwellian. On a sphere of radius 1, the potential is set to 1 (times T_e/e), representing essentially a non-plasma charge distribution whose shielding by the plasma is our interest. Particles move through this sphere without being absorbed. The simulation is initialized with uniform electron density and an equal and opposite fixed background charge density representing ions; there is therefore a full complement of trapped and untrapped particles, and the initial neutrality gives an initial potential $\propto 1/r$. The code is advanced forward in time with timesteps short enough to resolve the gyro-motion until a steady state is reached. In this final state the potential is shielded with characteristic length equal to ~ 1 (times λ_D). An example contour plot of potential in the plane $y = 0$ is shown in Fig. 2. It is almost exactly isotropic to within the noise level of the simulation (~ 0.01),

¹The velocity integral of a two-dimensional Maxwellian over $(v_x^2 + v_y^2) > 2\phi$ gives untrapped density exactly $n_{2u} = 1$, and the flat-trapped (integral over $(v_x^2 + v_y^2) < 2\phi$) density is $n_{2t} = \phi$, again giving a Boltzmann response $n_{2f} = (1 + \phi)$.

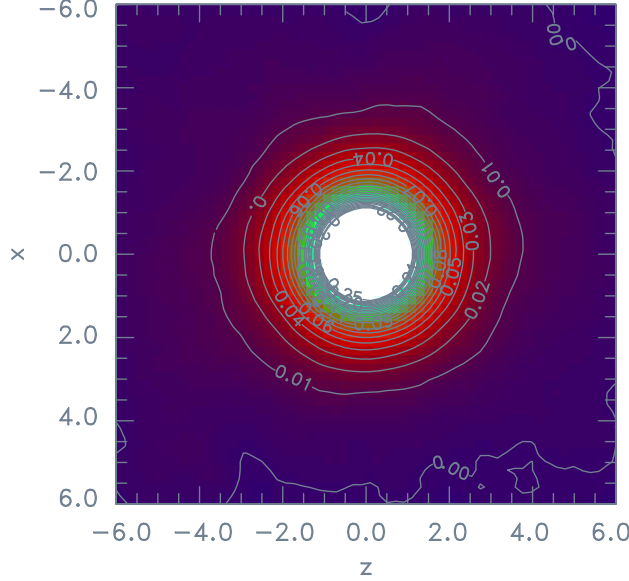


Figure 2: Potential contours around a non-absorbing equipotential surface (of unit radius and potential) show no significant anisotropy in a PIC simulation with $\omega_p/\Omega = 5$.

showing no sign of transverse elongation that would be present if anisotropic shielding such as eq. (5) applied. The extensive explored range of values $0.2 < \Omega/\omega_p < 2$ shows no tendency toward transverse elongation. Even oblate elliptical inner boundary shapes which enforce elongation at $r \sim 1$ have potential contours at larger radii that rapidly become spherical.

5 Asymptotic potential variation of an electron hole

We are now in a position to draw important conclusions about the form of the potential in the wings of an electron hole. The wings are what we call the spatial regions far enough from the hole center that the trapped particle deficit (meaning difference from “flat-trapped” distribution) is negligible. The crucial point is then that in the wings the density can be approximated as $n = 1 + \phi/\lambda_s^2$ (with no coordinate anisotropy), where λ_s is the effective shielding length (for stationary Maxwellian external distribution the Debye length, so $\lambda_s = 1$, but longer for fast-moving Maxwellians). The nonlinearity is weak because the potential is small so λ_s can be taken constant. Then the potential obeys the Modified Helmholtz Equation

$$\nabla^2 \phi - \phi/\lambda_s^2 = 0. \quad (8)$$

In other places where there is a trapped particle deficit, the resulting charge density perturbation enters as a source on the right-hand side.

One can represent the solution of the Modified Helmholtz equation in an infinite domain (isolated hole) as a sum of harmonics in the polar angle $\theta = \tan^{-1}(r/z)$. For a 2-D cartesian case where x is an ignorable coordinate, r corresponds to y , and $R^2 = y^2 + z^2$. The harmonics then are proportional to modified Bessel functions $e^{i\ell\theta} K_\ell(R/\lambda_s)$, whose asymptotic behavior is $K_\ell(\eta) \rightarrow \exp(-\eta)\sqrt{\pi/2\eta}$ for large argument η . For the cylindrical alternative

(axisymmetry about z) the harmonics are proportional to modified Spherical Bessel functions of argument $\eta = R/\lambda_s = (z^2 + r^2)/\lambda_s$ (where $r^2 = x^2 + y^2$), which are asymptotically proportional to $\sqrt{\pi/2\eta} K_{\ell+1/2}(\eta) = \exp(-\eta)\pi/2\eta$, and for $\ell = 0$ simply the familiar Yukawa potential. The mix of angular harmonics is determined by the angular dependence of the sources near $R = 0$, but the crucial point is that all of them decay radially predominantly as $\exp(-\eta)$; so $\frac{\partial\phi}{\partial R} \simeq -\phi/\lambda_s$. The *angular* component of the gradient is $\phi\ell/R$ which for low ℓ and large R becomes much smaller than $\frac{\partial\phi}{\partial R}$. Consequently, far from the charge sources in the hole, when $R \gg \lambda_s$ ($\eta \gg 1$) the potential decays mostly *radially* and $\propto \exp(-R/\lambda_s)$.

For a one-dimensional hole or a multidimensional hole near $r = 0$, the asymptotic parallel variation is $\phi \propto \exp(-z/\lambda_s)$ at large $|z|$; but also for any multidimensional hole shape, the asymptotic transverse variation is $\phi \propto \exp(-r/\lambda_s)$ near $z = 0$. These are physically inescapable asymptotes where trapped particles are negligible.²

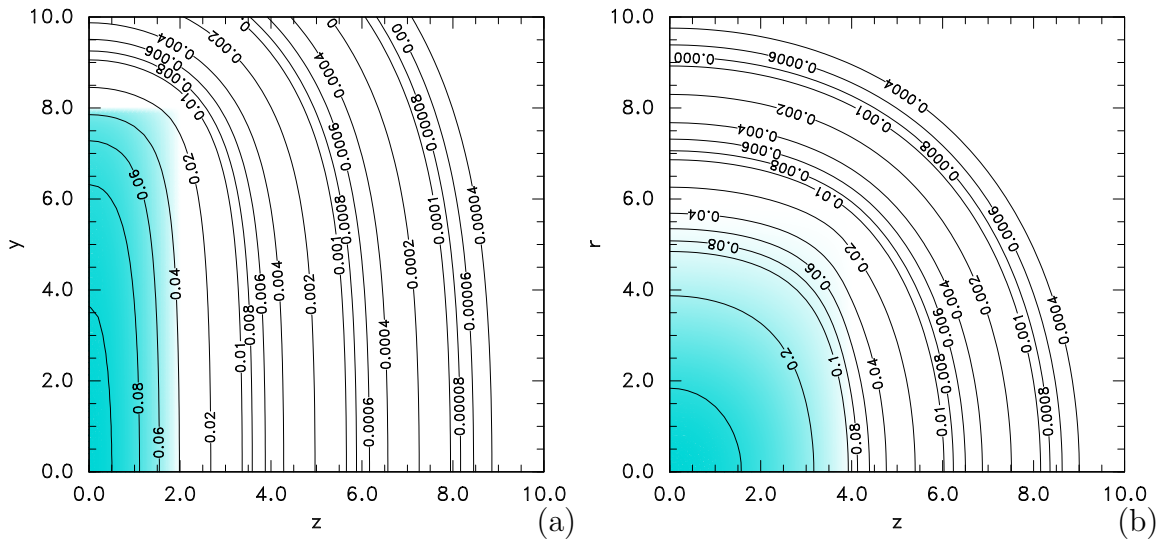


Figure 3: Examples of hole-like solutions of the Modified Helmholtz equation.

Figure 3 shows two examples of numerical solutions of the Modified Helmholtz equation on 2-D cartesian (left) (a), and axisymmetric (right) (b) domains with $\lambda_s = 1$. A specified additional charge source, representing trapped electron deficit (schematically, not self-consistently by actual trapping), is indicated by the blue color intensity on ϕ contour plots. Notice how the logarithmic ϕ contours are spaced (outside the shaded region) by the same distance at $z \sim 0$ as they are at $r, y \sim 0$, and that as we move further from the charge region the contours become increasingly circular. Also the logarithmic gradient (e.g. $-\partial \ln \phi / \partial r$ near $z = 0$) rises steeply as we move past the charge extent in the transverse direction (slightly overshooting and then) asymptoting to unity. These are universal qualitative features of such solutions. Of course, close-to or inside the blue (charge) region, the shape of the contours is strongly modified in accordance with the shape of the charge perturbation (just illustrative here); and it is the charge distribution that determines the resulting

²Gaussian potential shapes are frequently used in hole modelling, for mathematical convenience; and the choice is often justified as consistent with observations. However the observations so far reported have insufficient precision in the wings to distinguish between exponential and Gaussian asymptotic decay.

aspect ratio L_{\perp}/L_{\parallel} there. Oblate holes rely on their proximity to oblate distributions of trapped electron deficit for their shape, not on a supposed anisotropy of shielding arising from transverse polarization.

6 Conclusion

The empirical aspect ratio scaling of Franz et al $L_{\perp}/L_{\parallel} \simeq \sqrt{1 + \omega_p^2/\Omega^2}$ may represent a useful (though perhaps not universal) empirical fit to electron hole shapes in nature. But it cannot be explained by the equations of the “model” that they invoke because their anisotropic Poisson equation is based on a misunderstanding of polarization drift’s role and representation in gyrokinetic theory. It is shown here on general grounds that we can expect the electron hole potentials to decay essentially isotropically with local density approximately Boltzmann-like as $\phi \rightarrow 0$, corresponding to isotropic Debye screening. Charge density arising, for example, from trapped particle deficit is isotropically screened by untrapped particles. This is confirmed by simple PIC simulation. The wings of electron holes therefore are expected to have asymptotically exponential potential decay both parallel and perpendicular to the magnetic field.

Acknowledgements

I am grateful to Greg Hammett for several very helpful discussions on the foundations of gyrokinetic theory.

References

- [1] I H Hutchinson. Electron holes in phase space: What they are and why they matter. *Physics of Plasmas*, 24(5):055601, may 2017. URL <http://aip.scitation.org/doi/10.1063/1.4976854>.
- [2] I B Bernstein, J M Greene, and M D Kruskal. Exact nonlinear plasma oscillations. *Physical Review*, 108(4):546–550, 1957. URL <http://journals.aps.org/pr/abstract/10.1103/PhysRev.108.546>.
- [3] L Muschietti, I Roth, C W Carlson, and R E Ergun. Transverse instability of magnetized electron holes. *Physical Review Letters*, 85(1):94–97, 2000.
- [4] Mingyu Wu, Quanming Lu, Can Huang, and Shui Wang. Transverse instability and perpendicular electric field in two-dimensional electron phase-space holes. *Journal of Geophysical Research: Space Physics*, 115(10):A10245, 2010.
- [5] I H Hutchinson. Transverse instability of electron phase-space holes in multi-dimensional Maxwellian plasmas. *Journal of Plasma Physics*, 84:905840411, 2018. URL <http://arxiv.org/abs/1804.08594>.

- [6] I. H. Hutchinson. Transverse instability magnetic field thresholds of electron phase-space holes. *Physical Review E*, 99:053209, 2019.
- [7] I H Hutchinson. Electron phase-space hole transverse instability at high magnetic field. *Journal of Plasma Physics*, 85(5):905850501, 2019.
- [8] D B Graham, Yu V Khotyaintsev, A Vaivads, and M André. Electrostatic solitary waves and electrostatic waves at the magnetopause. *Journal of Geophysical Research: Space Physics*, 121:3069–3092, 2016.
- [9] K. Steinvall, Yu. V. Khotyaintsev, D. B. Graham, A. Vaivads, P.-A. Lindqvist, C. T. Russell, and J. L. Burch. Multispacecraft analysis of electron holes. *Geophysical Research Letters*, 46(1):55–63, 2019. URL <https://agupubs.onlinelibrary.wiley.com/doi/abs/10.1029/2018GL080757>.
- [10] A. Lotekar, I. Y. Vasko, F. S. Mozer, I. Hutchinson, A. V. Artemyev, S. D. Bale, J. W. Bonnell, R. Ergun, B. Giles, Yu. V. Khotyaintsev, P.-A. Lindqvist, C. T. Russell, and R. Strangeway. Multisatellite mms analysis of electron holes in the earth’s magnetotail: Origin, properties, velocity gap, and transverse instability. *Journal of Geophysical Research: Space Physics*, 125(9):e2020JA028066, 2020. URL <https://agupubs.onlinelibrary.wiley.com/doi/abs/10.1029/2020JA028066>. e2020JA028066 10.1029/2020JA028066.
- [11] J R Franz, P M Kintner, C E Seyler, J S Pickett, and J D Scudder. On the perpendicular scale of electron phase-space holes. *Geophysical Research Letters*, 27(2):169–172, 2000.
- [12] V. E. Zakharov and E. A. Kuznetsov. Three-dimensional solitons. *Zh. Eksp. Teor. Fiz*, pages 594–597, 1974.
- [13] W W Lee. Gyrokinetic approach in particle simulation. *Physics of Fluids*, 26:556–562, 1983.
- [14] D Jovanović, P K Shukla, L Stenflo, and F Pegoraro. Nonlinear model for electron phase-space holes in magnetized space plasmas. *Journal of Geophysical Research: Space Physics*, 107(A7):1–6, 2002.
- [15] M. Berthomier, R. Pottelette, L. Muschietti, I. Roth, and C. W. Carlson. Scaling of 3d solitary waves observed by fast and polar. *Geophysical Research Letters*, 30:SSC 4.1–5, 2003.
- [16] I. Y. Vasko, O. V. Agapitov, F. S. Mozer, A. V. Artemyev, J. F. Drake, and I. V. Kuzichev. Electron holes in the outer radiation belt: Characteristics and their role in electron energization. *Journal of Geophysical Research: Space Physics*, 122(1):120–135, 2017.
- [17] I. Y. Vasko, V. V. Krasnoselskikh, F. S. Mozer, and A. V. Artemyev. Scattering by the broadband electrostatic turbulence in the space plasma. *Physics of Plasmas*, 25(7):072903, 2018.

- [18] J. C. Holmes, R. E. Ergun, D. L. Newman, N. Ahmadi, L. Andersson, O. Le Contel, R. B. Torbert, B. L. Giles, R. J. Strangeway, and J. L. Burch. Electron Phase-Space Holes in Three Dimensions: Multispacecraft Observations by Magnetospheric Multiscale. *Journal of Geophysical Research: Space Physics*, 123(12):9963–9978, 2018.
- [19] Y. Tong, I. Vasko, F. S. Mozer, S. D. Bale, I. Roth, A. V. Artemyev, R. Ergun, B. Giles, P. A. Lindqvist, C. T. Russell, R. Strangeway, and R. B. Torbert. Simultaneous Multispacecraft Probing of Electron Phase Space Holes. *Geophysical Research Letters*, 45(21):11,513–11,519, 2018.
- [20] H. S. Fu, F. Chen, Z. Z. Chen, Y. Xu, Z. Wang, Y. Y. Liu, C. M. Liu, Y. V. Khotyaintsev, R. E. Ergun, B. L. Giles, and J. L. Burch. First measurements of electrons and waves inside an electrostatic solitary wave. *Physical Review Letters*, 124:095101, 2020.
- [21] John A. Krommes, W. W. Lee, and C. Oberman. Equilibrium fluctuation energy of gyrokinetic plasma. *The Physics of Fluids*, 29:2421, 1986.
- [22] G. W. Hammett, W. Dorland, and F. W. Perkins. Fluid models of phase mixing, landau damping, and nonlinear gyrokinetic dynamics. *Physics of Fluids B*, 4:2052, 1991.
- [23] Ya. L Al’pert, A V Gurevich, and L P Pitaevskii. *Space Physics with Artificial Satellites*. Consultants Bureau, New York, 1965.
- [24] J G Laframboise. Theory of Spherical and Cylindrical Langmuir Probes in a Collisionless Maxwellian Plasma at Rest. Technical Report 100, (Doctoral Dissertation) University of Toronto Institute for Aerospace Studies, 1966.
- [25] J G Laframboise and L J Sonmor. Current collection by probes and electrodes in space magnetoplasmas: A review. *Journal of Geophysical Research*, 98(A1):337–357, 1993.
- [26] Martin Lampe, Glenn Joyce, and Gurudas Ganguli. Analytic and Simulation Studies of Dust Grain Interaction and Structuring. *Physica Scripta*, T89(1):106, 2001. URL <http://www.physica.org/xml/article.asp?article=t089a00106.xml>.
- [27] I H Hutchinson and L Patacchini. Computation of the effect of neutral collisions on ion current to a floating sphere in a stationary plasma. *Physics of Plasmas*, 14(1):13505, 2007. URL <http://link.aip.org/link/PHPAEN/v14/i1/p013505/s1{&}Agg=doi>.
- [28] V L Krasovsky, H Matsumoto, and Y Omura. Effect of trapped-particle deficit and structure of localized electrostatic perturbations of different dimensionality. *Journal of Geophysical Research: Space Physics*, 109(A4):A04217, 2004.
- [29] I H Hutchinson. Nonlinear collisionless plasma wakes of small particles. *Phys. Plasmas*, 18:032111, 2011.